CHAPTER IV

Electrical Conductivity Response of Poly(phenylene vinylene)/Zeolite Composites Exposed to Ammonium Nitrate

Jirarat Kamonsawas[a], Anuvat Sirivat[a*], Pimpa Hormnirun[b], Walaiporn Prissanaroon[c]

[a] *The Petroleum and Petrochemical College, Chulalongkorn University, Bangkok, Thailand.*

[b] *Department of Chemistry, Faculty of Science, Kasetsart University, Bangkok, Thailand.*

[c] *Department of Industrial Chemistry, Faculty of Applied Science, KMITNB, Bangkok, Thailand.*

Abstract

Poly(p-phenylene vinylene) (PPV) was chemically synthesized via the polymerization of p-xylene-bis(tetrahydrothiophenium chloride) monomer and doped with H_2SO_4. In order to improve electrical conductivity sensitivity of the conductive polymer, Zeolites Y (Si/Al = 5.1, 30, 60, 80) are added into the conductive polymer matrix. All samples show definite positive responses towards NH_4NO_3. The sensitivities of the composite sensors increase linearly with increasing Si/Al ratio. The electrical sensitivity values obtained are equal to 0.201, 1.37, 2.80 and 3.18, respectively. The highest electrical conductivity sensitivity of materials is obtained with the doped PPV/Zeolite Y (Si/Al = 80); it is higher than that of PPV/Zeolite Y (Si/Al = 5.1). The difference in the interaction between NH_4NO_3 molecules and the sensing composites on the electrical sensitivity has been investigated by using doped PPV/Zeolite Y (Si/Al = 5.1, 30, 60, 80, H^+) as a model though the IR measurements.

Keywords: Conductive polymer, Gas sensor, Poly(p-phenylene vinylene), Ammonium nitrate, Zeolite Y

*Corresponding author. Tel.: +66 2218 4131; fax: +66 2215 4459.
E-mail address:* anuvat.s@chula.ac.th (A. Sirivat).

1. Introduction

Semiconductor gas sensors are widely used in both domestic and industrial applications due to their favorable characteristics such as low cost and the increasing demand for energy. The combustion of petroleum products such as diesel oil, heating oil, and heavy fuel oil generates pollutant emissions in the environment. Air pollution is the main environmental problem for all cities. Most toxic gases, for example, carbon monoxide (CO), can cause chest pain in heart patients, headaches, nausea and reduced mental alertness. Sulfer dioxide (SO_2) can induce a lung disease and breathing problems for asthmatics. Emission of sulfur dioxide also leads to the deposition of acid rain and other acidic compounds over long distances often more than 1,000 kilometers from their source. Such deposition changes the chemical balance of soils which can lead to the leaching of trace minerals and nutrients critical to trees and plants. In addition to those toxic gases present in atmosphere, terrorist bomb explosions are a factor of main concern; we need to develop a safe method to detect in advance the potential explosion via tailored gas sensors which can sense various volatiles of bomb chemicals, such as cyclotrimethylenetrinitramine (RDX), trinitrotulene (TNT), and ammonium nitrate [1] [2] [3] [4].

Conducting polymers such as poly(*p*-phenylene vinylene) (PPV) can serve as an active sensing material in devices because PPV possesses good optical and electrical properties, and it can be synthesized by a relative simple technique. To obtain an analyte-specific material the sensors should have very narrow chemical specificity with high sensitivity towards polar chemicals [5] [6] [7]. A zeolite is chosen as a selective microporous adsorbent to be introduced into a polymer matrix in order to increase sensitivity towards NH_4NO_3 [8] [9] [10].

2. Experiment Section

2.1 Materials

α,α'-dichloro-p-xylene, tetrahydrothiophene and methanol (Aldrich) were used to synthesize p-xylene-bis(tetrahydrothio- phenium chloride) monomer. Sodium hydroxide (Merck) and Hydrochloric acid (Merck) were used as the basic and the acidic reagents, respectively. Sulfuric acid (Merck) was used as the oxidant. Zeolite:

CVB100 (Si/Al = 5.1, NH$_3^+$) (Zeolyst), CVB300 (Si/Al = 5.1, Na$^+$) (Zeolyst), CVB400 (Si/Al = 5.1, H$^+$) (Zeolyst), CVB720 (Si/Al = 30, H$^+$) (Zeolyst), CVB760 (Si/Al = 60, H$^+$) (Zeolyst), CVB780 (Si/Al = 80, H$^+$) (Zeolyst) were used as the adsorbents. Ammonium hydroxide (Suksapan) and nitric acid (Fluka) were used to make ammonium nitrate (NH$_4$NO$_3$) which was the target chemical. Nitrogen (N$_2$, TIG) was used as the surface cleaning gas and to vaporized ammonium nitrate. All chemicals were used without further purifications.

2.2 Poly(p-phenylene vinylene) Synthesis and Doping Process

Synthesis of the p-xylene-bis(tetrahydrothiophenium chloride) monomer was achieved by reacting α,α'-dichloro-p-xylene with tetrahydrothiophene[11]. The precursor sulfonium polyelectrolyte was prepared in an aqueous solution by the base induced polymerization of an appropriate *bis*-sulfonium monomer. The polymerization reaction was terminated by the addition of dilute aqueous hydrochloric acid to the reaction mixture which was then dialyzed against water in order to separate the high molecular weight fraction from the monomeric and oligomeric residues as well as the sodium and chloride ions. Poly(p-phenylene vinylene) was essentially obtained by heating poly(p-xylene-bis(tetrahydrothiophenium chloride)) under vacuum at 180 °C for 6 hr [11]. The 18 M Sulfuric acid was used as a dopant solution at the mole ratios between PPV repeating unit per sulfuric acid equal to 1:1, 1:50, 1:100, 1:200, and 1:300. The doping process occurred after adding the dopant solution to a polymeric powder, and it was monitored by observing the color changes of powder from bright yellow to black [12].

2.3 Composite Preparation

PPV/Zeolite composites were prepared by dry mixing PPV particles with the zeolites at a volume ratio equal to 10:90. The composites were compressed into a disc form by using a hydraulic press at pressure equal to 6 kN.

2.4 Characterization

The FT-IR spectrometer (Bruker, model FRA 106/S) was used to characterize functional groups. A thermogravimetric analyzer (Dupont, model TGA 2950) with a heating rate 10 $^{\circ}$C/min under N_2 atmosphere was used to characterize PPV precursor, PPV, and doped PPV. An X-ray diffractometer (Rigaku, model D/MAX-2000) was used to determine the degrees of crystallinity of PPV and doped PPV, and the crystal orders of zeolites. A scanning electron microscope (SEM, JEOL, model JSM-5200) was used to study the morphology of PPV, doped PPV, Zeolites, and PPV/Zeolite composites at the magnifications of 1500 and 5000 and at 15 kV. The BET (Sorptomatic-1990) was used to measure the pore sizes and the surface areas of the zeolites. A custom made two-point probe with linear geometric array was used to measure the specific electrical conductivity of each sample.

2.5 Electrical Conductivity and Gas Measurements

The electrical conductivity of the PPV pellets under exposure to air, N_2 and NH_4NO_3 were measured by using the custom made two-point probe which was connected to a voltage supplier (Keithley, 6517A) in which its voltage was varied and the resultant current was measured. The electrical conductivity was calculated by utilizing the equation: $\sigma = (I/KVt)$, where I is the measured current (A), V is the applied voltage (V), t is the thickness, and K is the geometric correction factor of the two-point probe determined by calibrating the probe with a silicon wafer possessing a known resistivity value. The electrical conductivity response and sensitivity of the composites were determined by following the equations: $\Delta\sigma = \sigma_{NH4NO3} - \sigma_{N2,initial}$ and $\Delta\sigma / \sigma_{N_2\ initial}$, respectively. $\Delta\sigma$ is the difference in the specific electrical conductivity (S/cm), $\sigma_{N2,initial}$ is the specific electrical conductivity in N_2 before exposure (S/cm), and σ_{NH4NO3} is the specific electrical conductivity under NH_4NO_3 exposure (S/cm).

3. Results and Discussion

3.1. Characterization of Poly(p-phenylene vinylene).

FTIR spectra of PPV precursor, PPV, and sulfuric acid doped PPV were obtained. The presence of the absorption band near 960 cm^{-1}, resulting from C-H out-of-plane bending, is the characteristic of the trans configuration of the vinylene group [13]. The absorption band at 3022 cm^{-1} is due to the trans vinylene C-H stretching mode [14]. The absorption band at 550 cm^{-1} can be attributed to the phenylene out-of-plane ring-bending [14]. The bands at 830 cm^{-1} and 1511 cm^{-1} are assigned to the para-phenylene ring C-H out-of-plane bending and the C-C ring stretching, respectively [14]. The bands at 2872 and 2960 cm^{-1} are attributed to the CH$_3$ symmetric and the CH$_3$ asymmetric deformation, respectively [14]. After the heat treatment under vacuum, the intensity of these last two bands decreases. The intensity of the absorption band near 3022 cm^{-1} increases due to the elimination of the tetrahydrothiopenyl group and HCl. The absence of the C-S linkage peak at 632 cm^{-1} from tetrahydrothiophene indicates the full conversion of the precursor after pyrolysis [14]. Upon the oxidation of PPV, the FTIR spectrum shows new bands at 1550, 1485, 1316, 1280, 1150, and 876 cm^{-1}. The emergence of these new bands in the spectra can related to the formation of the quinoid structures [15]. The quinoid structure is a result of a break of symmetry of the polymeric chain. Although the formation of the quinoid structure is evidently clear under doping, the bands connected with benzoid structure (undoped PPV) still survive after the doping process. Therefore, even for extensive oxidation, only a partial oxidation of the polymer takes place and the two structures coexist [15].

The thermal behavior of the conductive polymer was investigated by using the TGA technique. There are three transitions for the PPV precursor at between 80-150 °C, 150-230 °C, and 520-580 °C. The first one is due to the removal of the solvent from the polymer. The second transition, between 150-230 °C, is related to the elimination reaction, which yields tetrahydrothiophene and HCl and converts the PPV precursor to PPV. The third transition is attributed to the degradation reaction of the main chain [14]. After the pyrolysis of PPV precursor under vacuum for 6 hr, it has two transitions. The weight loss between 50-80 °C is due to the removal of the physically absorbed water. The transition temperature occurring at around 450-580

°C can be attributed to the decomposition of polymer. Therefore, TGA results also confirm that tetrahydrothiophene and HCl were eliminated from PPV precursor after the thermal treatment. The thermal behavior of sulfuric acid doped PPV shows three-steps weight loss. The weight loss around 50-105 °C is attributed to the diffusion of physisorbed water. The second step, 50-250 °C, is due to the loss of counterions of the dopant. The last step, 600-680 °C, is related to the degradation of polymer.

From XRD patterns, the interplanar spacing between aromatic groups can be identified with the peak at 24.38 Å for PPV. After chemically oxidized with H_2SO_4, doped PPV show two peaks at 20.58 Å and 28.30 Å which can be related to the layer of the dopant and the polymer chain, respectively [16]. The doping process does not disrupt the original orientation of the PPV crystallites and the crystalline phase was retained under the doping [24]. The particle size analysis gives the particle diameter of PPV and doped PPV of about 37.52 μm and 30.00 μm, respectively. The standard deviations are 0.71 μm and 1.57 μm, respectively. The apparent densities of PPV and doped PPV are about 1.17 g/cm^3 and 1.02 g/cm^3 with standard deviations of 0.12 g/cm^3 and 0.09 g/cm^3, respectively.

3.2. Characterization of Zeolite and Composites.

XRD patterns of Zeolites Y (Si/Al = 5.1, 30, 60, 80, H$^+$) covering angles between $2\theta = 5\text{-}90^O$ were obtained. The major peaks of the zeolites are consistent with those of previously published work [17]. The BET specific surface areas of zeolites Y (Si/Al = 5.1, 30, 60, 80, H$^+$) are about 868 ± 5.65, 780 ± 0.35, 761 ± 28.99 and 1204 ± 25.45 m^2/g, respectively. The pore sizes of zeolites Y (Si/Al = 5.1, 30, 60, 80, H$^+$) were analyzed by using the N_2 adsorption which turn out to be 10.755 ± 0.0025, 9.64 ± 0.0980, 10.724 ± 0.0254, and 10.073 ± 0.0212 Å, respectively. The apparent densities of zeolites Y (Si/Al = 5.1, 30, 60, 80, H$^+$) are about 2.0046 ± 0.34, 1.8331 ± 0.27, 2.0102 ± 0.07, and 2.0048 ± 0.36 g/cm^3. Figures 1 (a)-(d) show SEM images of dPPV/Zeolite Y (Si/Al=5.1, H$^+$), dPPV/Zeolite Y (Si/Al=30, H$^+$), dPPV/Zeolite Y (Si/Al=60, H$^+$) and dPPV/Zeolite Y (Si/Al=80, H$^+$) composites of various Si/Al ratios. Zeolite Y particles appear to possess the irregular shape of crystals and appear to be inhomogenoeusly dispersed in the polymer matrix [17].

3.3. Electrical Conductivity in Air and N_2

The specific conductivity measurements of PPV, 300:1dPPV, and composites under air and N_2 were carried out at 28 ± 1 °C, and at 1 atm. Table 2 shows the electrical conductivity values and the sensitivity ($\Delta\sigma/\sigma_{N2}$) in air and nitrogen of PPV, dPPV, and all our composites studied. For PPV and dPPV, the electrical conductivity values in air are 5.54×10^{-03} and 1.17×10^{3} S/cm; they decrease to 3.10×10^{-05} and 8.50×10^{-03} S/cm when air is replaced by N_2. The decrease by nearly an order of magnitude suggests that certain components of moisture in air are active in interacting with PPV and dPPV [18].

3.4. Electrical Conductivity Sensitivity of PPV, dPPV and Zeolite Y exposed to NH_4NO_3

The electrical response ($\Delta\sigma = \sigma_{NH4NO3} - \sigma_{N2initial}$ [S/cm]) of each sample was calculated by the difference between the saturated electrical conductivity when exposed to NH_4NO_3 and the steady state conductivity value when exposed to pure N_2 at 1 atm and 30 ± 2 °C. Due to appreciable differences in initial conductivity between various composites, the sensitivity (Sensitivity = $\Delta\sigma/\sigma_{N2}$), defined as the electrical conductivity response divided by the electrical conductivity when exposed to pure N_2, will be used for comparison purposes.

PPV and their oligomers have been shown to be useful as active materials for gas sensor. PPV can detect 8 types of organic solvent (chloroform, acetone, ethanol, ethyl acetate, toluene, hexane, acetic acid, methanol, diethyl ether); their sensitivity values are between 10 – 40 % [15]. In our work, we demonstrate further that PPV can detect NH_4NO_3 vapor, commonly found in fertilizer and explosive material industries [15].

When dPPV is exposed to NH_4NO_3 at 377 ppm, its conductivity increases and the equilibrium sensitivity value, $\Delta\sigma/\sigma$, is equal to 9.65×10^{-01}. The positive increment of the sensitivity upon exposed to NH_4NO_3 can be traced back to the doped a PPV-NH_4NO_3 interaction mechanism to be proposed, along with data tabulated in Table 2. NH_4NO_3 molecules act as a secondary dopant, a substance which is subsequently applied to the primary-doped polymer, where charge transfer

complex is formed between the polymer and the secondary dopant [19]. This results in a greater number of charges along the polymer backbone and a correspondingly larger sensitivity. A possible interaction mechanism of dPPV-NH$_4$NO$_3$ interaction is proposed, as shown in Fig.6 which will be later discussed [19].

The electrical conductivity values of Zeolites Y (Si/Al = 5.1, 30, 60, 80) in air are 3.37×10^{-5}, 3.86×10^{-3}, 3.86×10^{-3}, 2.97×10^{-3} S/cm; they decrease to 1.25×10^{-05}, 1.47×10^{-5}, 1.45×10^{-5}, 2.82×10^{-5} S/cm when air is replaced by nitrogen.

When Zeolites Y are exposed to NH$_4$NO$_3$ at 377 ppm, the conductivity values increase by one order of magnitude and the sensitivity values are 1.21×10^{-01}, 1.98×10^{-01}, 3.83×10^{-01}, 4.64×10^{-01}, respectively. With increasing Si/Al ratio, it appears that the increase in Si in the Zeolite Y structure facilitates the static interaction between oxygen on the Si molecule in the Zeolite Y and NH$_4$NO$_3$ [20]. Therefore, Zeolite Y at Si/Al ratio = 80 shows the highest sensitivity.

3.5. dPPV/Zeolite Y Composites and Electrical Conductivity Response to NH$_4$NO$_3$: Effect of Si/Al ratio

Four different Zeolites Y , Si/Al = 5.1, 30, 60, 80 with the corresponding specific surface areas of 868, 760, 780 ,1204 g/m^2 and median pore sizes of 10.75, 9.56, 10.74, 10.10 °A were used to investigate the effect of Si/Al ratio on the electrical conductivity response towards NH$_4$NO$_3$. Our fabricated composites of doped PPV/Zeolite-Y's (Si/Al =5.1, 30, 60, 80) all contain 90% by volume of respective Zeolites.

Figures 2a-2c show the temporal response of the composites studied: doped PPV/Zeolite-Y (Si/Al = 5.1, 30, 60, 80). The temporal induction times are 41, 34, 91, and 118 min, respectively. These are directly related to the accessibility and the number of available active sites for NH$_4$NO$_3$. The induction time increases with increasing amount of Si in the zeolite framework. The increase in Si/Al ratio corresponds to a greater volume of NH$_4$NO$_3$ available to interact with active sites or the negative charge on the polymer chain. The induction times of the composites are longer than those of pure Zeolites Y and they are comparable to that of the pristine PPV and dPPV; this indicates that Zeolites Y can effectively induce NH$_4$NO$_3$ to interact with the available sites and improve sensitivity of the pristine PPV and dPPV

[19]. Table 2 summarizes the induction times and the recovery times of our samples investigated.

Table 2 tabulates electrical conductivity sensitivities of doped PPV/Zeolite-Y's (Si/Al = 5.1, 30, 60, 80). Table 2 tabulates electrical conductivity values in air of the composites studied. σ_{air} values are 1.56×10^{-2}, 6.15×10^{-2}, 1.47×10^{-2}, 2.71×10^{-2} S/cm for the composites with zeolites Y. The electrical conductivity is reduced by nearly an order magnitude when the composites are exposed to N_2 atmosphere. When they are exposed to NH_4NO_3 at 377 ppm, the conductivity increases and the sensitivity values are 5.86×10^{-01}, 1.48, 2.52, 3.79, respectively for the composites with the zeolites Y (Si/Al = 5.1, 30, 60, 80). Hence, it appears that the composite PPV/Zeolite Y (Si/Al =80) has the highest sensitivity, whereas the composites PPV/Zeolite Y (Si/Al =5.1) possess the lowest sensitivity.

Figure 3 shows that all of the composites have larger sensitivity values than that of the pristine PPV, 5.55×10^{-02}, and doped PPV, 9.65×10^{-01}. The increase in the sensitivity values of PPV/Zeolite composites relative to that of the pristine PPV and doped PPV reflects the fact that NH_4NO_3 molecules can adsorb into the Zeolites by the electrostatics. Therefore, under this assumption, a larger amount of NH_4NO_3 molecules are available to interact with dPPV chains.

Figure 4 shows the structure of NH_4^+, Zeolite Y structure and interaction between NH_4^+ and Zeolite Y. Even through Zeolite Y (Si/Al =80) and Zeolite Y (Si/Al =5.1) have comparable specific surface area: 1204 and 868 g/cm^2. The higher surface area induces the target gas to reside in the cavity [20]. With increasing Si/Al ratio, it appears that the increase in Si in the Zeolite Y structure facilitates the static interaction between oxygen on the Si molecule in the Zeolite Y and NH_4NO_3. Increasing the static interaction between target gas and zeolite improves sensitivity of the PPV/ZeoliteY composites [21, 22].

3.6. FTIR investigations of reactions of adsorbed NH_4NO_3

FTIR spectra of PPV, dPPV, Zeolite Y and dPPV/Zeolite Y were taken . The . The spectra of samples were collected before, during at 15 minutes interval, and after NH_4NO_3 exposure, in order to study the interaction between the samples and NH_4NO_3.

IR spectra of NH_4NO_3 shows the 700-3500 cm^{-1} region identifying the NH_4NO_3 absorption at 1 atm and at room temperature. The vibrational stretching frequencies of free NH_4^+ molecule are ($v = 3330, 3300$ cm^{-1}) [20, 23] and of free NO_3^- molecule are ($v = 1300$-1350 cm^{-1}, 815-840 cm^{-1}) [24].

Figure 5 shows the IR spectrum of dPPV before NH_4NO_3 exposure, during NH_4NO_3 exposure, and after NH_4NO_3 exposure. Before NH_4NO_3 exposure, the IR spectrum shows a peak at 1170 cm^{-1} which is assigned to the quinoid structure, at 1519 and 3022 cm^{-1} which can be assigned to the phenylene characteristics [14, 15]. During NH_4NO_3 exposure, the IR spectrum shows a new peak at 3336 cm^{-1} which can be assigned to the vibration of NH_4^+ interacting with carbon cation on the quinoid structure of doped PPV [20, 23]. The two new peaks at 1333 and 830 cm^{-1} can be assigned to the vibration of NO_3^- interacting with cation on the quiniod structure of doped PPV [24]. Increasing intensity at wavenumber 1172 cm^{-1} during NH_4NO_3 exposure is caused by the increase in the quinoid structures in doped PPV. The intensities of peaks at 3019, 1517 cm^{-1} decrease after NH_4NO_3 exposure and the peaks at wavenumbers 3336, 1333 cm^{-1} disappear. The decreases of the intensities at wavenumbers 3019, 1517 cm^{-1} after NH_4NO_3 exposure confirm that NH_4NO_3 molecules may act as a secondary dopant and the number of the quinoid structures increases in dPPV [19]. This is the FTIR evidence for the previously proposed interaction schematic of Figure 6.

Figure 7 shows the IR spectra of Zeolite Y (Si/Al=5.1, H^+) before NH_4NO_3 exposure, during NH_4NO_3 exposure, and after NH_4NO_3 exposure. Before NH_4NO_3 exposure, the IR spectrum shows a peak at 3640 cm^{-1} which can be assigned to the silanol group [25]. During NH_4NO_3 exposure, the IR spectrum show new two peaks at 3334 and 1625 cm^{-1} which can be assigned to the NH_4^+ interacting with oxygen molecules on Si molecule [20, 23]. The new peak at 1380 cm^{-1} can be assigned to the NO_3^- interacting with oxygen molecules on Si molecule [24]. A peak at 3663 cm^{-1}, which can be assigned to characteristic of zeolite after NH_4NO_3 exposure, confirms that no interaction between the zeolite and NH_4NO_3 remains. There is no significant band pattern difference between the spectrum before and after exposed to NH_4NO_3 [27, 28, 29].

Figure 8 shows the IR spectra of NH_4NO_3 (pressure at 1 atm and at room temperature) adsorbed on dPPV/Zeolite-Y (Si/Al=80, H^+) before NH_4NO_3 exposure, during NH_4NO_3 exposure, and after NH_4NO_3 exposure. Before NH_4NO_3 exposure, the IR spectrum shows a peak at 1160 cm^{-1} which can be assigned to the quinoid structure, at 1517 and 3010 cm^{-1} which can be assigned to the phenylene characteristic[14, 15], and at 3660 cm^{-1} which can be assigned to the silanol group [25]. During NH_4NO_3 exposure, the IR spectrum shows a new peak at 3340 cm^{-1} which can be assigned to NH_4^+ interacting with cation on dPPV and oxygen on Si molecule [20, 23]. The new peak at 1330 cm^{-1} can be assigned to NO_3^- interacting with cation on dPPV and oxygen on Si molecule [24]. The intensities of the peaks at 3023, 1520 cm^{-1} decrease during and after exposure. The decreases of intensities at wavenumber 3023, 1520 cm^{-1} during and after exposure confirms that NH_4NO_3 molecules may act as a secondary dopant. The number of the quinoid structures increases in dPPV structure corresponding to the intensity increase at 1170 cm^{-1} during NH_4NO_3 exposure. After NH_4NO_3 exposure, the peaks at 3340, 1330 cm^{-1} disappear. A peak at 3663 cm^{-1} can be assigned to characteristic of zeolite after NH_4NO_3 exposure, confirms that no interaction between zeolite and NH_4NO_3 remains [29, 30]. This is the FTIR evidence for the previously proposed mechanism that Zeolite Y induces a larger volume of NH_4NO_3 vapor for interact with dPPV and NH_4NO_3 molecules may act as a secondary dopant. This clearly suggests that the interactions are further induced by the presence of Zeolite Y (Si/Al=80, H^+) [31, 32]. Figure 9 shows a schematic of the proposed interactions between NH_4NO_3 and dPPV/Zeolite-Y's

4. Conclusions

Doped PPV with H_2SO_4 is utilized as a NH_4NO_3 gas sensing material due to the positive response. The electrical conductivity sensitivity of 300:1 dPPV towards NH_4NO_3 can be improved by introducing zeolite Y into dPPV matrix. The sensitivity increases with Si/Al ratio up to 80. The effect of Si/Al ratio is then investigated, at ratios of 5.1, 30, 60 and 80. The sensitivity of the composites with different Si/Al ratios can be arranged in this order; dPPV/Zeolite Y (Si/Al=5.1, H^+) < dPPV/Zeolite Y (Si/Al=30, H^+) < dPPV/Zeolite Y (Si/Al=60, H^+) < dPPV/Zeolite Y (Si/Al=80,

H^+). The electrical sensitivity increases with increasing Si/Al ratio can be described in terms of the specific surface area, evidenced from the interaction on the IR spectra. The dPPV/Zeolite Y (Si/Al=80, H^+) possesses the highest sensitivity of 3.79 since Zeolite Y (Si/Al=80, H^+) has the highest specific surface area and it can induce the favorable NH_4NO_3 vapor adsorption on the composite. From FTIR investigation, the NH_4NO_3-dPPV interaction is irreversible while NH_4NO_3-zeolite interaction is reversible.

Acknowledgements

Table 1 Surface areas and pore volumes of zeolites

Zeolite	BET surface area (m^2/g)	Median Pore width (^oA)
Zeolite Y (Si/Al = 5.1, H^+)	864 ± 5.65	10.75 ± 0.0025
Zeolite Y (Si/Al = 30, H^+)	780 ± 0.35	9.56 ± 0.0982
Zeolite Y (Si/Al = 60, H^+)	740 ± 28.99	10.74 ± 0.0254
Zeolite Y (Si/Al = 80, H^+)	1222 ± 25.45	10.10 ± 0.0212

Table 2 The observed sensitivity and temporal response for NH_4NO_3 Adsorbed on PPV, doped PPV samples, Zeolite Y and dPPV/90%Zeolite Y

Sample	σ_{air} (S/cm)	$\sigma_{N2\,final}$ (S/cm)	$\Delta\sigma$ (S/cm)	Sensitivity ($\Delta\sigma/\sigma_{N2}$)	Temporal response (min)	Recovery time, t_r (min)
PPV	$5.54 \times 10^{-3} \pm 3.65 \times 10^{-3}$	$3.10 \times 10^{-5} \pm 8.06 \times 10^{-6}$	$2.00 \times 10^{-6} \pm 8.63 \times 10^{-8}$	$5.55 \times 10^{-2} \pm 9.84 \times 10^{-3}$	81 ± 38	28 ± 19
doped PPV	$1.17 \times 10^{3} \pm 1.36 \times 10^{-2}$	$8.50 \times 10^{-3} \pm 1.19 \times 10^{-2}$	$8.37 \times 10^{-3} \pm 1.18 \times 10^{-2}$	$9.65 \times 10^{-1} \pm 2.86 \times 10^{-2}$	80 ± 27	38 ± 25
Zeolite Y (Si/Al = 5.1, H^+)	$3.37 \times 10^{-5} \pm 7.01 \times 10^{-6}$	$1.25 \times 10^{-5} \pm 1.46 \times 10^{-6}$	$1.60 \times 10^{-6} \pm 4.71 \times 10^{-8}$	$1.21 \times 10^{-1} \pm 7.88 \times 10^{-3}$	88 ± 29	138 ± 38
Zeolite Y (Si/Al = 30, H^+)	$2.46 \times 10^{-3} \pm 2.54 \times 10^{-3}$	$1.47 \times 10^{-5} \pm 2.95 \times 10^{-6}$	$2.94 \times 10^{-6} \pm 8.50 \times 10^{-7}$	$1.98 \times 10^{-1} \pm 1.81 \times 10^{-2}$	103 ± 53	56 ± 21
Zeolite Y (Si/Al = 60, H^+)	$3.86 \times 10^{-3} \pm 3.33 \times 10^{-3}$	$1.45 \times 10^{-5} \pm 2.22 \times 10^{-6}$	$5.54 \times 10^{06} \pm 8.13 \times 10^{-7}$	$3.83 \times 10^{-1} \pm 2.55 \times 10^{-3}$	105 ± 28	25 ± 4
Zeolite Y (Si/Al = 80, H^+)	$2.97 \times 10^{-3} \pm 2.24 \times 10^{-3}$	$2.82 \times 10^{-5} \pm 6.37 \times 10^{-6}$	$1.15 \times 10^{-5} \pm 2.82 \times 10^{-6}$	$4.64 \times 10^{-1} \pm 2.15 \times 10^{-2}$	101 ± 21	48 ± 8
dPPV/90%Zeolite Y (Si/Al = 5.1, H^+)	$2.71 \times 10^{-2} \pm 1.79 \times 10^{-2}$	$2.83 \times 10^{-3} \pm 3.51 \times 10^{-3}$	$2.60 \times 10^{-3} \pm 3.57 \times 10^{-3}$	$5.86 \times 10^{-1} \pm 5.37 \times 10^{-1}$	41 ± 11	23 ± 8
dPPV/90%Zeolite Y (Si/Al = 30, H^+)	$6.15 \times 10^{-2} \pm 2.19 \times 10^{-3}$	$1.23 \times 10^{-4} \pm 1.24 \times 10^{-4}$	$1.73 \times 10^{-4} \pm 1.64 \times 10^{-4}$	$1.48 \times 10^{0} \pm 1.64 \times 10^{-1}$	34 ± 11	47 ± 14
dPPV/90%Zeolite Y (Si/Al = 60, H^+)	$1.47 \times 10^{-2} \pm 2.04 \times 10^{-3}$	$2.04 \times 10^{-3} \pm 7.83 \times 10^{-4}$	$1.61 \times 10^{-3} \pm 2.20 \times 10^{-3}$	$2.52 \times 10^{0} \pm 4.06 \times 10^{-1}$	91 ± 23	38 ± 6
dPPV/90%Zeolite Y (Si/Al = 80, H^+)	$1.56 \times 10^{-2} \pm 4.98 \times 10^{-3}$	$2.70 \times 10^{-5} \pm 1.14 \times 10^{-5}$	$9.73 \times 10^{-5} \pm 2.02 \times 10^{-5}$	$3.79 \times 10^{0} \pm 8.60 \times 10^{-1}$	118 ± 38	20 ± 10

σ = electrical conductivity values in air, N_2 and NH_4NO_3, $\Delta\sigma$ = the electrical response and $\Delta\sigma/\Delta\sigma_{N2}$ = electrical conductivity sensitivity, at $T=28\pm1$ °C, and at atmospheric pressure.

(a)

(b)

(c)

(d)
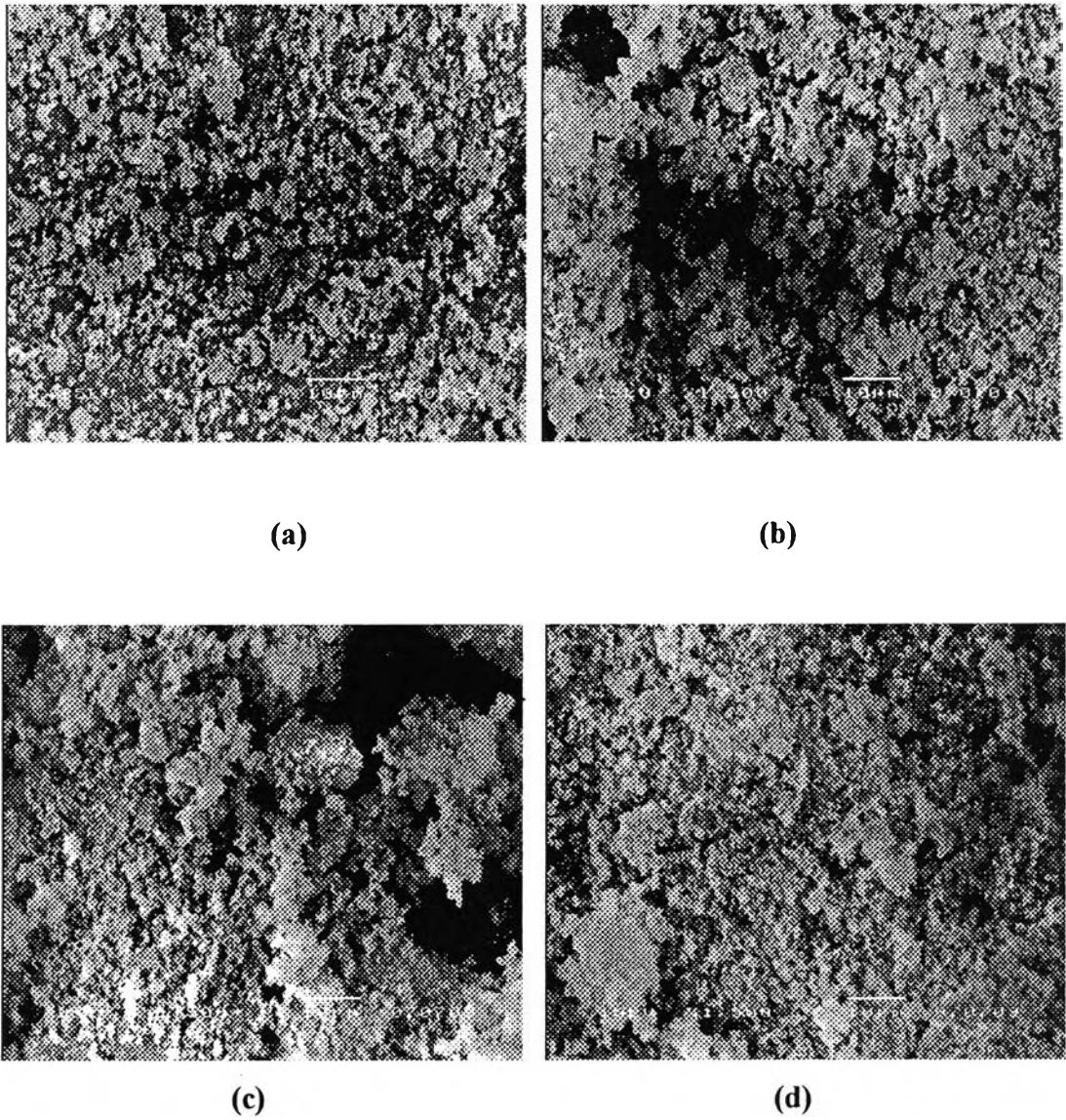
Fig. 1. SEM micrographs of powder samples at the magnification 1500, 15 kV of; (a) dPPV/Zeolite Y (Si/Al=5.1, H⁺); (b) dPPV/Zeolite Y (Si/Al=30, H⁺); (c) dPPV/Zeolite Y (Si/Al=60, H⁺); (d) dPPV/Zeolite Y (Si/Al=80, H⁺).
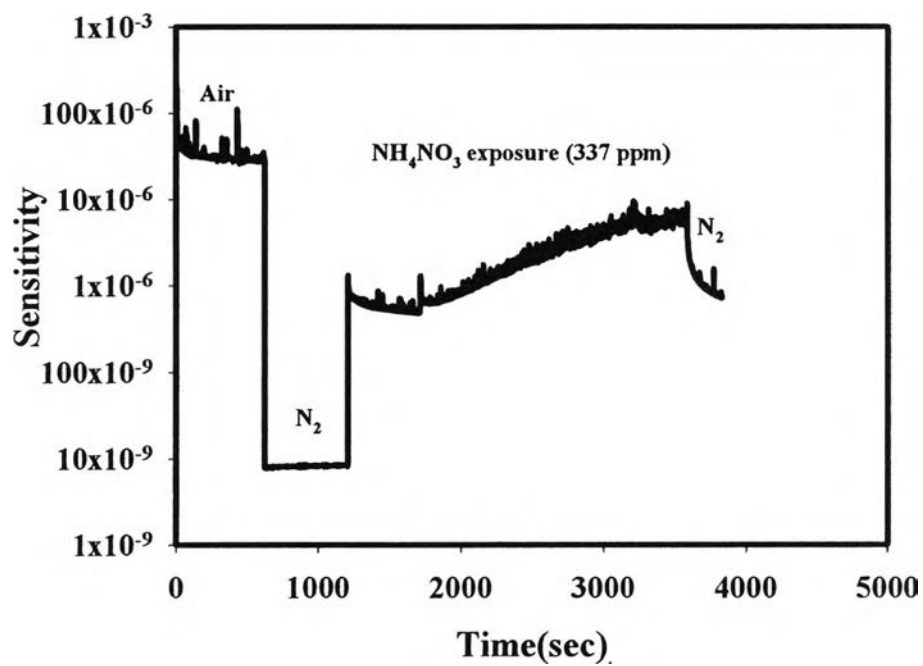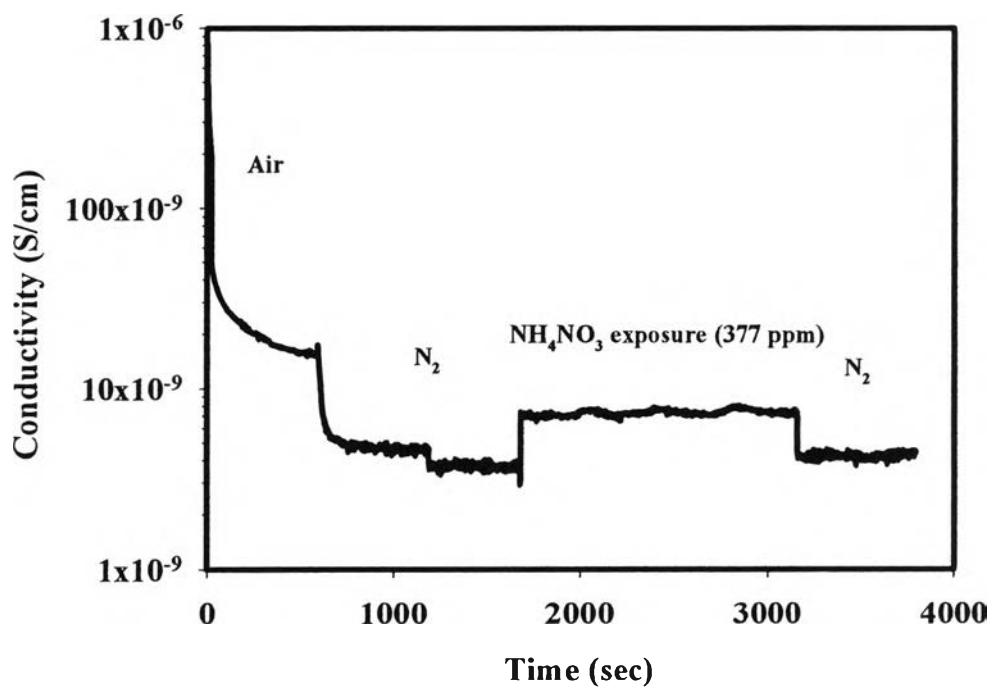
Fig. 2a. The response of doped PPV.
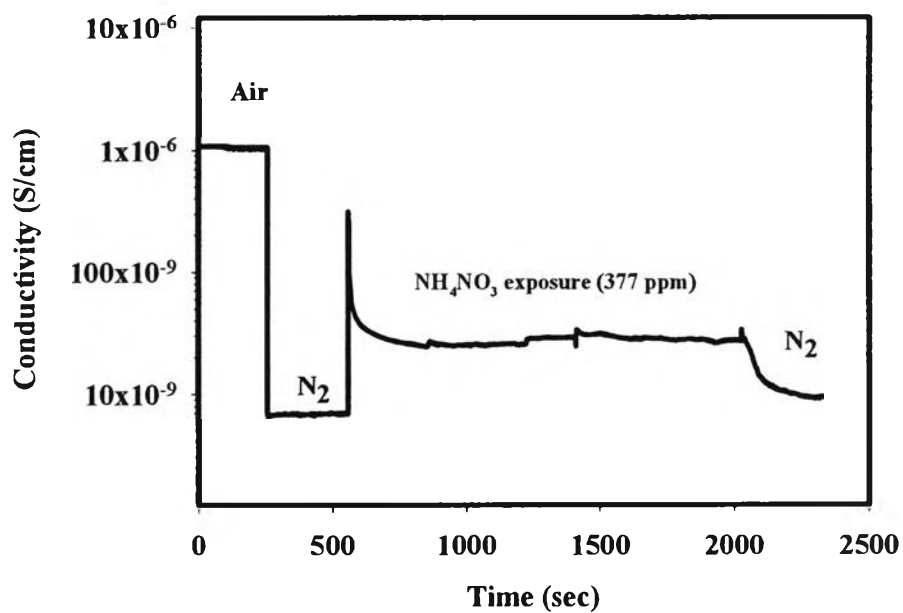

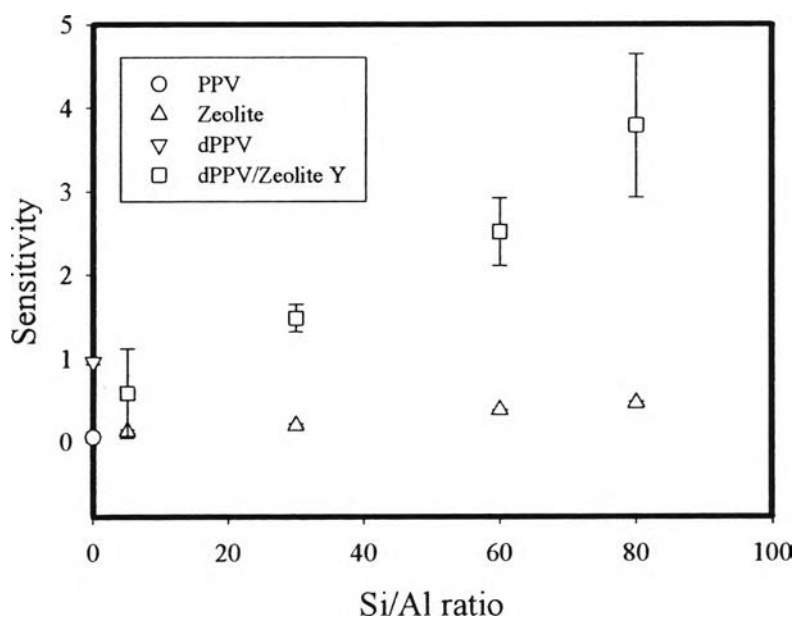**Fig. 2b.** The response of Zeolite Y.
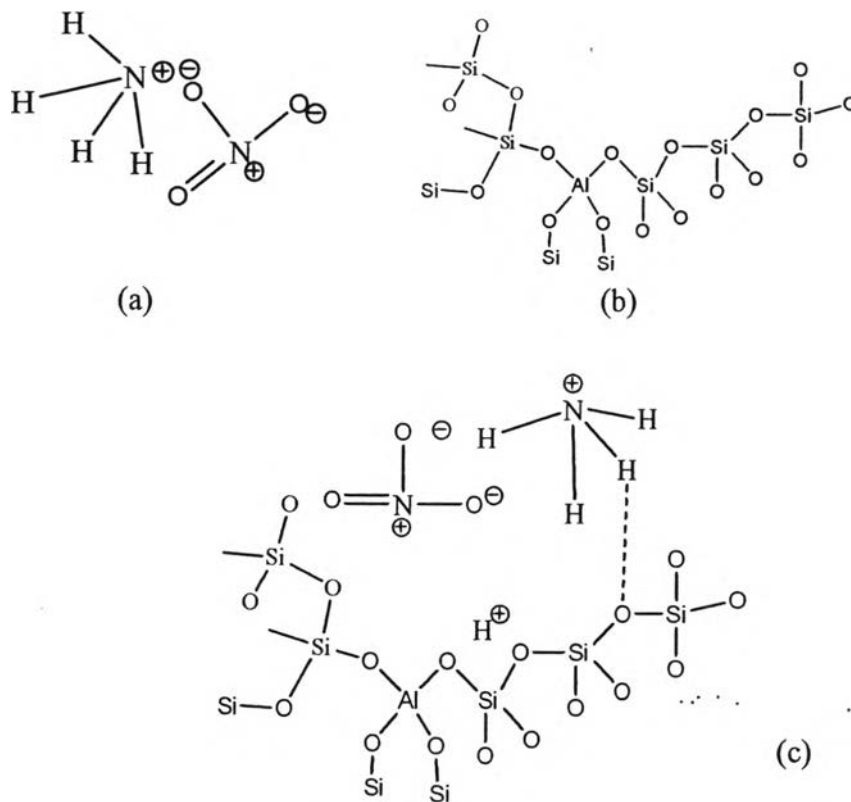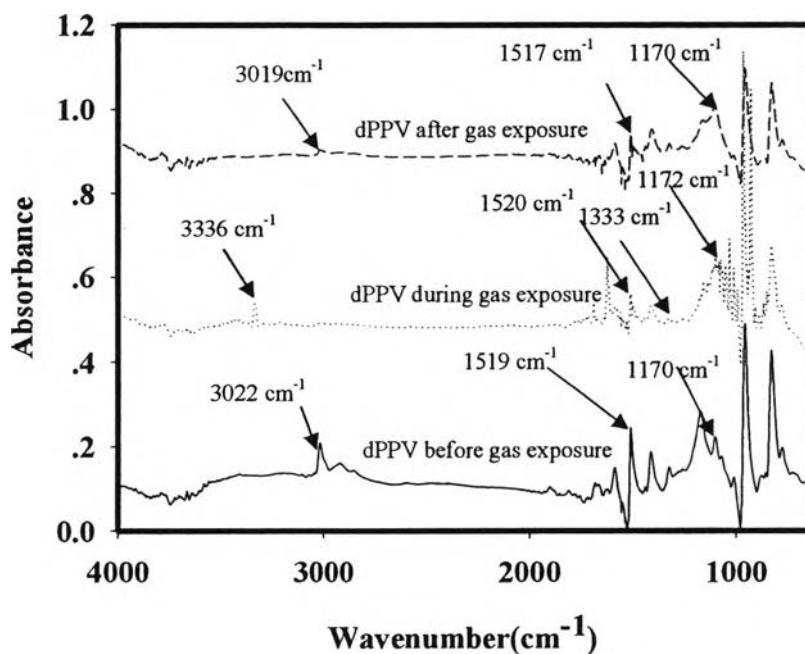
Fig. 2c. The response of dPPV/Zeolite Y.
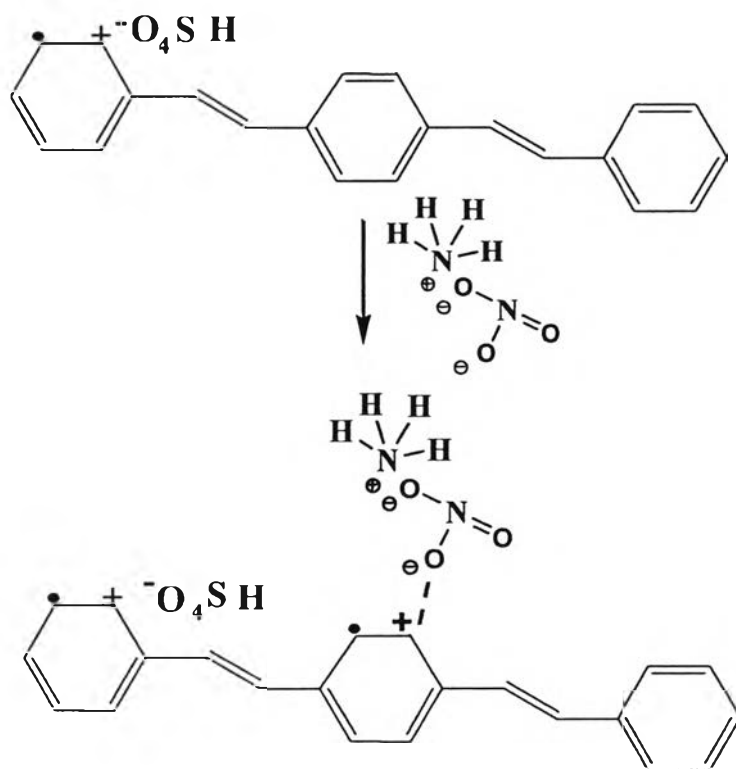

Fig. 3. Sensitivity of PPV, dPPV, Zeolite Y and dPPV/zeolite Y.

Fig. 4. The structure of: (a) NH_4NO_3; (b) Zeolite Y structure; and; (c) interaction between NH_4NO_3 and Zeolite.

Fig. 5. IR spectra of doped PPV exposed to NH_4NO_3 (NH_4NO_3=0.0377 % v/v, pressure at 1 atm and at T=25°C).

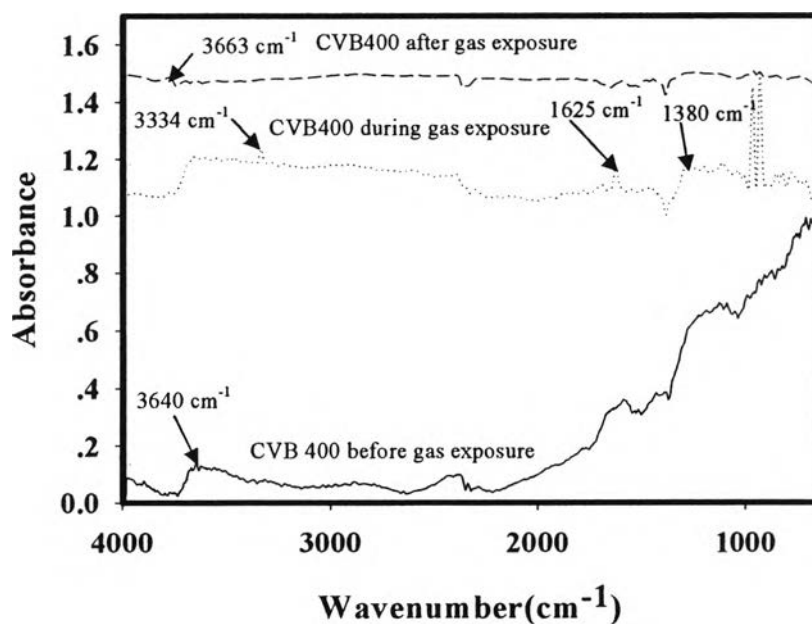**Fig. 6.** Proposed mechanism of the NH_4NO_3-dPPV.

Fig. 7. IR spectra of Zeolite Y (Si/Al=5.1, H⁺) exposed to NH_4NO_3 (NH_4NO_3=0.0377 % v/v, pressure at 1 atm and at T=25°C).
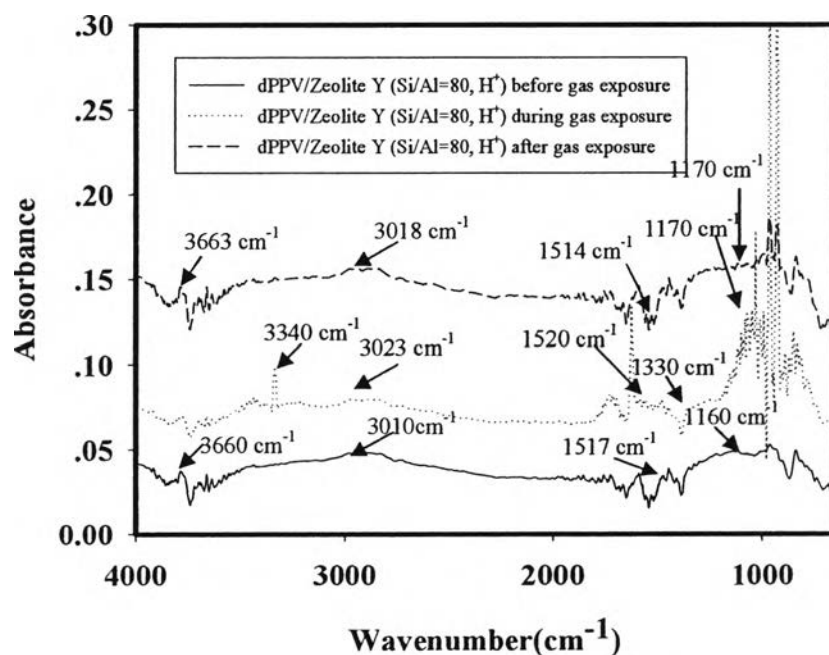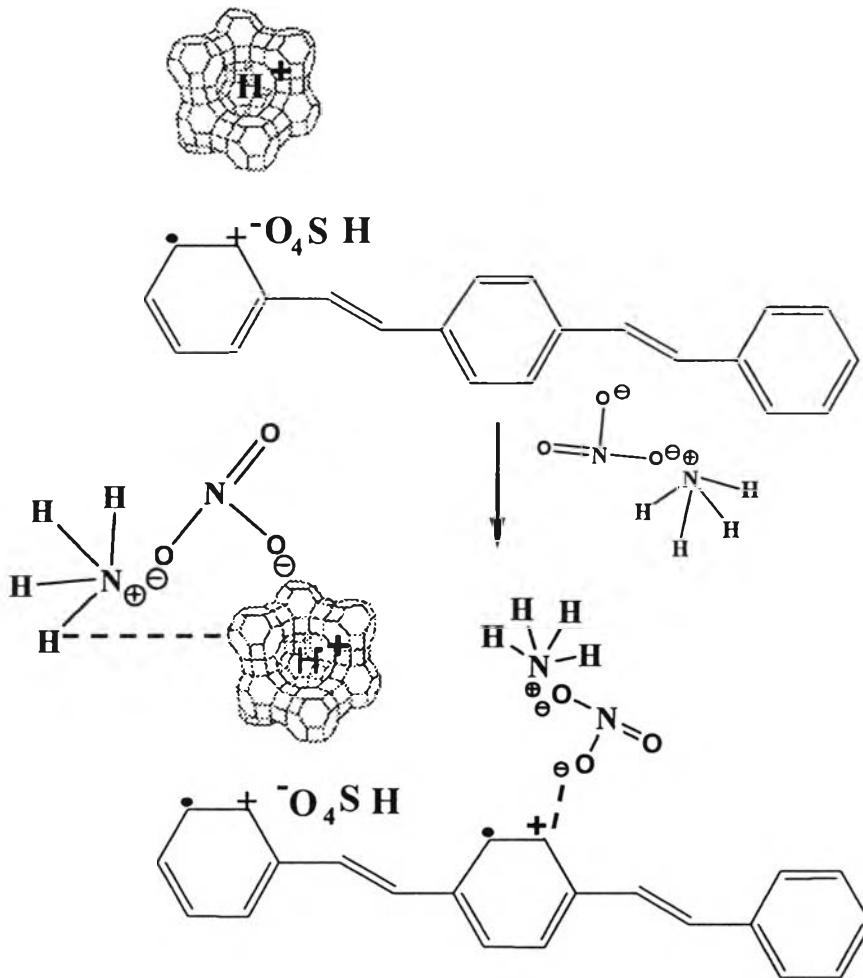

Fig. 8. IR spectra of dPPV/Zeolite Y (Si/Al=80, H⁺) exposed to NH_4NO_3 (NH_4NO_3=0.0377 % v/v, pressure at 1 atm and at T=25°C).

Fig. 9. Show the schematic of the proposed interactions between NH_4NO_3 and the doped PPV/ Zeolite Y.

REFERENCES

[1]   G.E. Collins, L.J. Buckley, Conductive polymer coated fabrics for chemical sensing, Synthetic Metals 78 (1996) 93-101.

[2]   J.H. Alan, A.D. Maria, Semiconducting polymers as a material for photonic device, Solid state and Materials Science 3 (1998) 16-22.

[3]   A.J. Heeger, Semiconducting and Matallic polymers:the fourth generation of polymeric materials, Synthetic metal 125 (2002) 23-42.

[4]   K.C. Persaud, Polymer in chemical sensing, Material Today 8 (2005) 38-44.

[5]   F. Babudri, *et al.*, Deposition and application in gas sensors of thin films of a bridged chain dialkoxy PPV derivative, Material Science and Engineering 22 (2002) 445-448.

[6]   R. Bouchet, S. Rosiri, *et al.*, Solid state hydrogen sensor based on acid doped polybenzimidazole, Sensors and Actuators B 76 (2001) 610-616.

[7]   F. Babudri, *et al.*, Deposition and application in gas sensors of thin films of a bridge chain dialkoxy PPV derivative, Material Science and Engineering 22 (2002) 445-448.

[8]   S.C. Graham, *et al.*, High sensitivity radiation sensing by photo induced doping in PPV derivatives, Synthetic Matals 102 (1999) 1169-1170.

[9]   G. Hagen, A. Dubbe, *et al.*, Selective impedance based gas sensors for hydrocarbons using ZSM-5 zeolite films with chromium (3) oxide interface, Sensors and Actuators B 119 (2006) 441-448.

[10]   M. Vilaseca, J. Coronas, *et al.*, Gas detection with SnO2 sensors modified by zeolite films, Sensors and Actuators B, 124 (2007) 99-110.

[11]   R.A. Wessling, *et al.*, U.S. Patent 561 (1996) 706.

[12]   M. Ahlskog, M. Reghu, T. Noguch, B. Ohnishi, B., Doping and conductivity studies on poly (p-phenylene vinylene). Synthetic Metal 89 (1997) 11-15.

[13]   D. R. Gagnon, J. D. Capistran, F. E. Karasz, R. W. Lenz and S. Antoun, Synthesis, doping, and electrical conductivity of high molecular weight poly(p-phenylene vinylene), Polymer 28 (1984) 567-573.

[14]   A.Cirpan, Z. Kucukyavuz, S. Kucukyavuz, Synthesis, characterization and electrical conductivity of poly (paraphenylene vinylene), Turkish Polym. J 27 (2003) 135-143

[15]   L.O. Peres, R. Mauro, B. Fernandes , R. Jarem, B. Garcia, S.H. Wang, C. Francisco, B. Nart, Synthesis and characterization of chloro and bromo substituted p-phenylene vinylene homopolymers and alternating copolymers, Synthetic Metals 156 (2006) 529–536.

[16]   J. M. Madsen, B. R. Johnson, X. L. Hua, R. B. Hallock, M. A. Masse and F. E. Karasz, Temperature dependence of the electrical conductivity of AsF_5-doped poly(p-phenylene vinylene), The American Physical Society 40 (1989) 11751-11755.

[17]   D.W. Break, *Zeolite Molecular Sieves*; Robert E. Krieger Publishing; Florida, 1973.

[18]   C. Chuapradit, L.R. Wannatong, D. Chotpattananont, A. Sirivat, J. Schwank, Polyaniline/zeolite LTA composites and electrical conductivity, Polymer 46 (2005) 947–953.

[19]   N. Densakulprasert, W. Ladawan, C. Datchanee, P. Hiamtup, A. Sirivat, and J. Schwank, Electrical conductivity of polyaniline/zeolite composites and synergetic interaction with CO, Materials Science and Engineering B 117 (2005) 276-282.

[20]   A. Zecchina, L. Marchese, S. Bordiga, C. Paze, and E. Gianotti, Vibrational Spectroscopy of NH_4^+ Ions in Zeolitic Materials: An IR Study 101 (1997) 10128-10135.

[21]   K. Thuwachaosoan, D.Chotpattananont, *et al.*, Electrical conductivity responses and interactions of poly(3-thiopheneacetic acid)/zeolites L, mordernite, beta and H_2. Material Science and Engineering B (2007)

[22]   B. Soontornworajit, L. Wannatong, P. Hiamtup, S. Niamlang, D. Chotpattananont, A. Sirivat, J. Schwank, Induced interaction between polypyrrole and SO_2 via molecular sieve 13X, Materials Science and Engineering B 136 (2007) 78–86.

[23]   A. Zecchina, F. Geobaldo, C. Lamberti, G. Ricchiardi, S. Bordiga, P.G. Turnes Palomino, Reply to Comments on "N_2 Adsorption at 77 K on H-Mordenite and Alkali-Metal-Exchanged Mordenites: An IR Study", J. Phys. Chem 48 (1996) 18883.

[24]   A. Matsumoto, T. Kitajima, K. Tsutsumi, Adsorption Characteristics and Polymerization of Pyrrole on Y-Zeolites, Langmuir 15 (1999) 7626-7631.

[25]   N. Venkatathri, Synthesis and characterization of high silica content silicoaluminophosphate SAPO-35 from non-aqueous medium, Catalysis Communications 7 (2006) 773-777.

[26]   Y. Kuroda, Y. Yoshikawa, Characterization of specific N_2-adsorption site existing on CuZSM-5 type zeolite: effect of ion-exchange level on adsorption properties, The Journal of Physical Chemistry B 103 (1999) 2155-2164

[27]   J.C. Yang, P.K. Dutta, Promoting selectivity and sensitivity for a high temperature YSZ-based electrochemical total NOx sensor by using a Pt loaded zeolite Y filter, Sensors and Actuators B, (2007

[28]   C.L. Angell, Carbon Dioxide Adsorbed on Linde X and Y Zeolites, J. Phys. Chem. 70 (1966) 1413.

[29]   C. Schmidt, T. Sowade, E. Loffler, A. Birkner, W. Grunert, Preparation and structure of In-ZSM 5 catalysts for the selective reduction of NO by hydrocarbon, The Journal of Physical Chemistry B 106 (2002) 4085-4097.

[30]   K. Gaare, D. Akporiaye, Effects of La Exchange on NaY and NaX Zeolites as Characterized by ^{29}Si NMR, The Journal of Physical Chemistry B 101 (1997) 48-54.

[31]   M.K. Ram, *et al.*, CO gas sensing from ultrathin nano-composite conducting polymer film. Sensors and Actuators B 106 (2006) 750-757.